JOURNAL OF AGRICULTURAL AND FOOD CHEMISTRY

Nonenzymatic Browning Kinetics of a Carbohydrate-Based Low-Moisture Food System at Temperatures Applicable to Spray Drying

SONG MIAO AND YRJÖ H. ROOS*

Department of Food and Nutritional Sciences, University College Cork, Ireland

Effects of water contents on nonenzymatic browning (NEB) rates of amorphous, carbohydrate-based food model systems containing L-lysine and D-xylose as reactants were studied at different temperatures (40, 50, 60, 70, 80, and 90 °C) applicable to spray drying conditions. Water sorption was determined gravimetrically, and data were modeled using the Brunauer−Emmett−Teller and Guggenheim−Anderson−deBoer equations. Glass transition, T_g was measured by DSC. NEB was followed spectrophotometrically. The rate of browning increased with water content and temperature, but a lower $T - T_g$ was needed for browning at decreasing water content. Water content seemed to affect the activation energy of NEB, and higher water contents decreased the temperature dependence of the NEB. At higher temperatures, the NEB became less water content dependent and enhanced browning in spray-drying. The temperature dependence of nonenzymatic browning could also be modeled using the Williams−Landel−Ferry (WLF) equation, but the WLF constants were dependent on the water content.

KEYWORDS: Nonenzymatic browning; water content; temperature; model

INTRODUCTION

Nonenzymatic browning (NEB, Maillard reaction) is one of the most important chemical reactions in foods. Maillard reaction is known to generate flavor compounds, including characteristic flavors and colors of thermally processed and prepared foods (*1*). It also produces high-molecular-weight colored products known as melanoidins, which are responsible for the brown color and the products of the browning reactions of many foods. Nonenzymatic browning affects the nutritional quality and toxicological properties of food materials. Both flavor generation and browning can be favorable or unfavorable (*2*), especially in dairy products. The extent of Maillard reaction can be optimized through careful manipulation of processing and storage conditions (*3*). Therefore, control of the NEB reaction rate during processing and storage has been given much attention.

In an effort to optimize processing and storage conditions of dry and intermediate moisture foods, increasing attention has been paid to understanding effects of physical properties of food materials on NEB kinetics (*4*−*12*). Spray-drying is a typical dehydration method in food and pharmaceutical industries producing amorphous materials. The physical stability of amorphous food materials can be related to glass transition (*13*−*15*). Below glass transition, molecules have very slow mobility and they are fixed in the highly viscous, nonequilibrium, solid-like, glassy state (*14*, *16*). Above glass transition, the viscosity of the material decreases dramatically because of thermal or water plasticization. Diffusion-controlled chemical reactions, including nonenzymatic browning, in low and intermediate-moisture foods are dependent on translational diffusivity of the reactants, and presumably, on the viscosity of the matrix material. Such reactions have been suggested to be dependent on the physical state of the system (*13*, *14*, *17*−*20*).

Studies relating nonenzymatic browning and physical state have concentrated on the examination of the effects of changes in matrix materials on reaction rates. The effects of the glass transition on NEB rates have been studied using different model systems over various temperature ranges (*6*, *8*, *11*, *12*, *19*−*23*) and at a constant temperature at various water contents and water activities (*7*, *10*, *19*, *22*−*24*). Particular attention has been paid to the effects of different $T - T_g$ conditions (*19*, *21*−*23*) and concomitant physical changes, such as collapse or crystallization (*6*, *7*, *10*, *11*, *19*) and also the type and concentration of reactants (*3*, *5*, *12*). All these studies have revealed the independent effects of glass transition and macroscopic changes in amorphous materials on the nonenzymatic browning rates.

Spray-drying is a common method in the dairy industry. During the spray-drying process, concentrated liquids are dehydrated in the form of tiny droplets. The physical state of the material changes from liquid to solid as it passes through the drying chamber. The time for the product changing from the liquid state to an amorphous solid powder is extremely short, and the particle temperature is not likely to increase extensively during dehydration. Most of the wet particles experience only

* To whom correspondence should be addressed. Tel.: +353-21-4902386. Fax: +353-21-4270213. E-mail: yrjo.roos@ucc.ie.

10.1021/jf049706t CCC: $27.50
Published on Web 07/14/2004

the wet bulb temperature during the drying of 95% of the water, and therefore, thermal changes (e.g., NEB) may be avoided for most powder products. However, further heating of the amorphous particles at final stages of dehydration and in a collecting chamber can be relatively long and important in controlling the final quality of the products. Although, in most modern spray-drying operations, powders are removed quickly to allow rapid cooling. However, a given population of particles may experience quick drying and exposure to the hot drying air for a relatively long time. Hence, the particle temperature may increase quickly, which is likely to cause "burning" of spray-dried particles, affecting the quality of the final products.

Most of the kinetic data for the nonenzymatic browning reaction at different water contents and temperatures have been determined by use of model food systems such as polyvinylpyrrolindone (PVP)- and maltodextrin (MD)-based food models. These food models have different properties from real lactose-based dairy products. Roos and others (*15*) quantified the rate of water formation from the T_g depression to determine the kinetics of the NEB reaction at different temperatures. So far, there have been only a few studies reporting browning rates in dairy powder systems at high temperatures and specific water contents applicable to spray-drying conditions. In the present study, a food model with physical properties, such as the glass transition behavior, typical of lactose-based dairy powder products was developed. The objective was to relate temperature and water content with the extent of browning over a typical spray drying temperature range and to evaluate the effects of temperature and water content on browning kinetics.

MATERIALS AND METHODS

Preparation of the Model System. An amorphous food model consisting of lactose (Sigma Chemical Co., St. Louis, MO) and trehalose (British Sugar Company, UK) (1:1) as matrix materials was prepared. The major constituent of a number of dried dairy-based powders is lactose. The model system had a similar type glass transition behavior as lactose because of the very similar glass transition behavior of the two sugars. However, crystallization of component sugars was delayed in this system. L-lysine (Sigma) and D-xylose (Sigma) were used as nonenzymatic browning reactants, because of their high reactivity (*19*). According to the results of previous studies (*9*, *25*) and pre-experiments carried out in the present study, the exact amounts of the reactants, 1:1, were adjusted to 5% (w/w) of the total solids. The compositions of the model system were lactose 45%, trehalose 45%, xylose 5%, and lysine 5% (w/w) of the total solids. A 20% (w/w solids) clear solution was prepared from the matrix materials, the reactants, and distilled water. Solutions in 20−22 mL aliquots were frozen on Petri dishes immediately after preparation (24 h at −20 °C, followed by 24 h at −80 °C) and freeze-dried (>48 h, $p < 0.1$ mbar) (Lyovac GT 2; Amsco Finn-Aqua Gmbh, Hürth, Germany), to produce a completely amorphous glassy state of the food model (*13*).

The freeze-dried materials were ground immediately after freeze-drying. Ground powders on Petri dishes were exposed in vacuum desiccators to three relative vapor pressures (RVP) of water, as reported by Roos and Karel (*13*), to adjust water contents of the materials. Three saturated salt solutions (LiCl, CH_3COOK, and $MgCl_2$) (Sigma Chemical Co.) were used to achieve RVP values of 11.4, 23.1, and 33.2%, respectively (*26*, *27*). The exposure time was 72 h. Thereafter, aliquots of 1 g of each material were transferred into glass ampules (5-mL gold band ampule, WHEATON, Millville, NJ) and the ampules were stored in vacuum desiccators over the same respective RVPs for another 24 h. Then, ampules were flame-sealed by use of an acetylene flame. Because the 5-mL glass ampule has a small headspace, we presumed that during present NEB study the moisture contents of the samples in the ampules maintained constant, and more importantly, we presumed a homogeneous vapor pressure with the samples during experiment.

Sorption Isotherms. Sorption isotherms for the food model were determined gravimetrically. Triplicate samples of 1 g of the freeze-dried food model, prepared in 20-mL glass vials, were stored in a vacuum desiccator over P_2O_5 (Sigma Chemical Co.) for a week. After storage, the samples were considered "anhydrous". The dehydrated triplicate samples were subsequently kept at 23−24 °C over saturated solutions of LiCl, CH_3COOK, $MgCl_2$, K_2CO_3, $Mg(NO_3)_2$, $NaNO_2$, and NaCl (Sigma Chemical Co.) with RVP of 11.4, 23.1, 33.2, 44.1, 54.5, 65.6, and 76.1%, respectively (*26*, *27*), until the sample weights leveled off, indicating steady-state water contents. The samples were weighed at 3, 6, 9, 11, 21, and 24 h and then at 24-h intervals for RVP ≤ 44.1%. For ≥ 54.5% RVP, samples were weighed every hour up to 6 h, then 8, 10, 21, and 24 h and then at 24-h intervals during storage. All vials were kept closed with caps after the vacuum was released in the desiccators prior to weighing. The Brunauer−Emmett−Teller (BET) (*28*, *29*) and Guggenheim−Anderson−deBoer (GAB) (*29*, *30*) sorption isotherm models were fitted to the water sorption data using linear regression and quadratic analysis, as described by Jouppila and Roos (*31*).

Moisture Content Determination. As a result of sorption of water from the environment during sample preparation to the ampules, the water contents of the samples kept in sealed ampules varied slightly. Therefore, the water sorption data were used to predict water contents. The water activity of samples kept in sealed ampules was measured with an AquaLab CX-2 (Decagon Devices, Inc. Pullman, WA) water activity meter. Six samples of each material were measured, and the water contents were calculated using the GAB isotherm model.

Differential Scanning Calorimetry. Differential scanning calorimetry (DSC, Mettler Toledo 821e) was used to measure glass transition temperatures (T_g) for dehydrated and rehumidified samples as described by Lievonen et al. (*8*). Samples (9−15 mg) were prepared in preweighed DSC aluminum pans (40 μL; Mettler Toledo-27331, Switzerland) and stored in open pans for 144 h at room temperature in evacuated desiccators over P_2O_5 and different saturated salt solutions: LiCl, CH_3COOK, $MgCl_2$, K_2CO_3, (Sigma Chemical Co.) with RVP of 11.4, 23.1, 33.2 and 44.1%, respectively, giving a water activity, a_w, of 0.01 × RVP at equilibrium (*27*). RVP of the saturated salt solutions were confirmed with an AquaLab CX-2 (Decagon Devices) water activity meter. After equilibration, the pans were hermitically sealed. Triplicate samples of each material were analyzed. An empty pan was used as a reference. The DSC was calibrated for temperature and heat flow by use of indium (mp, 156.6 °C, ΔH_m, 28.45 J/g), *n*-pentane (mp, −129.7 °C, ΔH_m, 116.7 J/g), *n*-hexane (mp, −94.0 °C, ΔH_m, 151.8 J/g), distilled water (mp, 0.0 °C, ΔH_m, 334.5 J/g), and gallium (mp, 28.9 °C, ΔH_m, 80 J/g). The samples were scanned first over the glass transition range at 5 °C/min, then cooled at 10 °C/min to at least 30 °C below the glass transition, and a second heating scan at 5 °C/min was run to at least 30 °C above the glass transition. Samples with various water contents were scanned in hermetically sealed pans. Glass transitions were analyzed using STAR^e thermal analysis software, version 6.0 (Mettler Toledo, Switzerland). The glass transition temperature, T_g, was taken from the onset temperature of the glass transition temperature range. An average obtained for three replicate samples was taken as the glass transition temperature.

The Gordon and Taylor (*32*) equation (eq 1) was fitted to the experimental T_g data

$$T_g = \frac{w_1 T_{g1} + k w_2 T_{g2}}{w_1 + k w_2} \quad (1)$$

where w_1 and w_2 are the weight fractions of the solute and water respectively, T_{g1} is the T_g of anhydrous solute, T_{g2} is the T_g of amorphous water, and k is a constant. The T_g of −135 °C was used for water (*33*). The value for k was the mean derived from the experimental data on T_g and water content, as described by Jouppila and Roos (*31*). Equation 1 was applied in the present study for predicting water plasticization of the lactose/trehalose/reactant mixtures, considering that all solid components contributing to the observed glass transition were miscible and formed a single phase (*34*). Because serious browning occurred at high temperatures above 100 °C, water produced in the reaction plasticized the samples (*15*). Hence, no reliable glass transition temperature (T_g) could be measured for the anhydrous lactose/trehalose/reactant system. We assumed that the low concentration of reactants

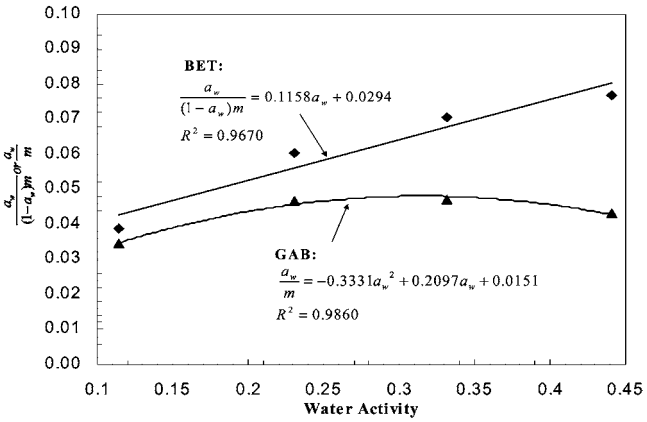

Figure 1. Calculation of the BET and GAB isotherm parameters, with the experimental sorption data using linear regression and quadratic analysis.

only slightly affected the T_g, and we used the T_g of the lactose/trehalose system as the T_g for the anhydrous lactose/trehalose/reactant system. When the Gordon and Taylor equation was used, the glass transition temperatures, T_g, of the model samples with different water contents could be predicted.

Nonenzymatic Browning. The flame-sealed ampules were stored at 10 °C intervals at six temperatures over the range of 40−90 °C, which was considered applicable to droplet and particle temperatures at spray-drying conditions. Duplicate samples were removed at 5−15 min intervals, depending on storage temperature, and subsequently stored at −80 °C, to avoid further browning before analysis. The extent of browning was determined spectrophotometrically (Perkin-Elmer Lambda 2 UV−Vis spectrometer; Morwalk, CT). The optical density (OD), which is used to detect products of early stages of browning (*35*) and is considered to result from the formation of furfural compounds (*36*, *37*), was measured at 280 and 420 nm for yellow and brown pigments, respectively (*38*). Samples were dissolved with 40 mL of distilled water and diluted when necessary, to obtain reliable absorbance readings. NEB was modeled as a zero-order reaction, as often reported in the literature (*5*). Rate constants, *k*, their 95% confidence limits, and coefficients of determination (R^2) were calculated by use of a linear regression analysis, as recommended by Labuza (*39*).

RESULTS AND DISCUSSION

Water Sorption. The model system was very hygroscopic. Both the BET and GAB isotherms could be used to model the experimental data (**Figure 1**). Experimental water sorption values, as a function of water activity at 25 °C, for the food model are given in **Figure 2B**. The BET and GAB monolayer values at 25 °C were 6.8 and 4.0 g of H_2O/100 g of solids, respectively. Compared to that of lactose, as shown in **Figure 2A**, the model system had similar sorption properties. Parameters for the BET and GAB isotherms for freeze-dried food model system and lactose are given in **Table 1**. Sorbed water contents of the model food system (3.3, 5.0, 7.0, and 10.2 g/100 g dry solids) were very close to that of pure lactose (2.8, 5.0, 6.6, and 9.7 g/100 g dry solids) when the model was exposed to RVP of 11.4, 23.1, 33.2, and 44.1%. At higher RVPs from 54.5 to 76.1%, both the model system and lactose showed increasing sorption of water, followed by a decrease in sorbed water content, as a result of sugar crystallization (*31*, *40*, *41*). As shown in **Figure 2**, when samples were exposed to RVP ≥ 54.5%, sorbed water contents were very low. This was because, as a result of crystallization component, component sugars released sorbed water (*34*). Compared to the water contents of lactose at RVP ≥ 54.4% (**Figure 2A**), the water contents of the model system (**Figure 2B**) were higher. Our model system contained trehalose, which may form dihydrate crystals, and

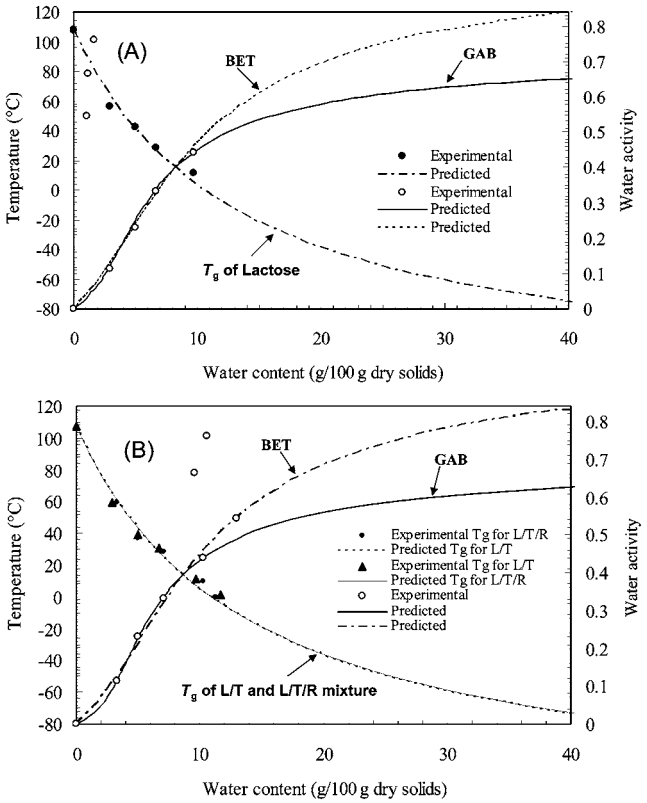

Figure 2. Sorption isotherm of (**A**) lactose and (**B**) lactose/trehalose/reactant- (L/T/R) based food model, with xylose and lysine (5% of solid, 1:1) as reactants, and the relationship between glass transition temperature (T_g), water content, and water activity for the model system.

after crystallization, the dihydrate trehalose crystals hold more water than lactose monohydrate or anhydrous crystals do. In the mix of lactose and trehalose, the crystallization of the component sugars was significantly delayed. First, the model system sorbed more water (13.1, 19.3, and 25.3 g/100 g of dry solids) than pure lactose (9.9, 11.3, and 13.2 g/100 g of dry solids) before showing the loss of sorbed water at RVP of 54.5, 65.6, and 76.1%. Second, the loss of sorbed water in model system was observed after 300, 56, and 32 h of storage, and in pure lactose after 11, 4, and 3 h of storage at RVP of 54.5, 65.6, and 76.1%. These results showed that in the selected model system, crystallization of component sugars was delayed. This was an important requirement for the study of the NEB kinetics in amorphous or at least partially amorphous models at different temperatures. In fact, when the humidified model samples were sealed in the DSC pans and exposed to the highest temperature for the longest time period, glass transition for the sample was still observed, which confirmed that amorphous material was remaining in the samples. The delayed crystallization of the component sugars in our present study was in agreement with the results of Arvanitoyannis and Blanshard (*42*) and Biliaderis et al. (*43*).

Because the GAB model is generally accepted to model water sorption of foods, and it is applicable over a wide a_w range (*29*, *30*), it was used to predict water contents at various browning conditions; the GAB model was used to calculate the water contents for the model samples with known water activity.

Glass Transition Temperature. The glass transition temperature of the food model decreased with increasing water content (**Figure 2**), which was typical of materials plasticized by water (*14*, *29*). The decrease was similar to that of other biological materials (*14*). The glass transition behavior of the

Table 1. Modeling Constants and Monolayer Value, m_m, for the GAB and BET Isotherms in Freeze-Dried Food Model System and Freeze-Dried Lactose

BET Model

	a_w range[a]	n^b	b	c	K	m_m	$R'^{2\,d}$
freeze-dried model	0.114–0.441	4	0.1158	0.0294	4.9388	6.89	0.967
freeze-dried lactose	0.114–0.441	4	0.1123	0.0358	4.1369	6.75	0.9502

GAB Model

	a_w range[a]	n^b	α	β	γ	C	K'	m_m	$R^{2\,c}$
freeze-dried model	0.114-0.441	4	-0.3331	0.2097	0.0151	1.4393	11.6488	3.95	0.9860
freeze-dried lactose	0.114-0.441	4	-0.2972	0.1407	0.0288	1.3872	7.5439	4.05	0.9988

[a] a_w range of experimental sorption data. [b] Number of experimental data points. [c] R^2 for the quadratic regression $(a_w/m) = \alpha a_w^2 + \beta a_w + \gamma$. [d] R'^2 for the linear regression $(a_w/m\,(1 - a_w)) = ba_w + c$.

Table 2. Glass Transition Temperatures of the Freeze-Dried Model System, Lactose, and Lactose/Trehalose Mixtures Stored for 144 h at Various Relative Vapor Pressure (RVP) at Room Temperature (22–23 °C)

	RVP	glass transition temperature (deg C)		
salt	(% of water)	freeze-dried L/T/R	freeze-dried L/T	freeze-dried L
LiCl	11.4	59.74 ± 0.12	59.78 ± 0.25	56.61 ± 0.42
CH_3COOK	23.1	36.88 ± 0.19	39.51 ± 0.04	42.42 ± 0.32
$MgCl_2$	33.2	28.82 ± 0.25	30.48 ± 0.15	28.41 ± 0.21
K_2CO_3	44.1	9.61 ± 0.09	11.67 ± 0.33	11.24 ± 0.44
$Mg(NO_3)_2$	54.5	0.17 ± 0.36	1.56 ± 0.38	

Table 3. Water Activity, Predicted Water Content, and Corresponding Predicted Glass Transition Temperature of the Food Model System

water activity[a] (A_w ± SD)	water content, predicted by GAB model (g/100 g solid)	water content, predicted by BET model (g/100 g solid)	predicted T_g[b] (deg C)
0.146 ± 0.006	3.78	3.69	55.0
0.279 ± 0.008	5.85	6.27	34.8
0.330 ± 0.012	6.86	7.27	26.4

[a] Each value is an average of six samples. [b] T_g was predicted by the Gordon and Taylor equation.

lactose/trehalose/reactant model system was similar to that of lactose and the lactose/trehalose mixture (**Table 2**), although the food model had slightly lower T_g values at the same water contents. This was probably due to additional plasticization of the lactose/trehalose mixture by xylose and lysine. The experimental glass transition temperatures, T_g, of the food model over the a_w range of 0−0.441 were successfully predicted by eq 1 (**Figure 2B**). The constant, k, for the model system and lactose was 7.3 ± 0.7 and 7.7 ± 0.8, respectively, which was close to the value (6.7) reported by Jouppila and Roos (*31*) for freeze-dried lactose. From the experimental water activity data for the food model exposed to different RVP environments, glass transition temperatures and water contents were predicted, as shown in **Table 3**. The predicted T_g of the food model at $0.33a_w$ was 26.4 °C, which was very close to the experimental value (28 °C) at $0.332a_w$.

NEB. The rate of the nonenzymatic browning reaction at the three different water contents of the model systems increased with increasing temperature. The rate obtained from increasing optical density at 280 nm was higher than that at 420 nm, and it was typical of that of food models with low and intermediate water contents (*44*). Plots of optical density against storage time showed an initial induction lag period for all samples at different temperatures. This was followed by a linear increase in optical

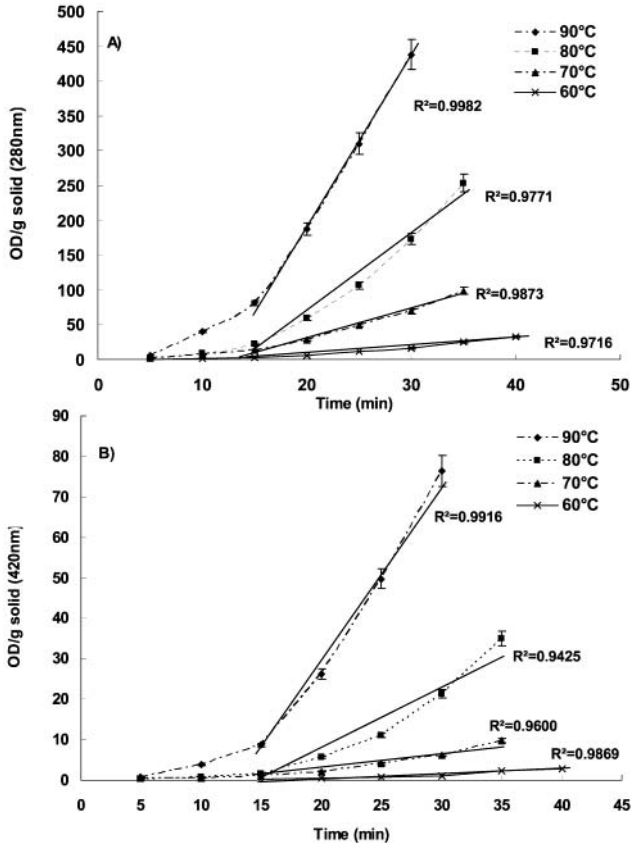

Figure 3. Optical density of lactose/trehalose/reactant food model (water content: 6.86 g water/100 g of dry solids) at (**A**) 280 nm and (**B**) 420 nm against time at different temperatures. Regression lines with coefficients of determination (R^2) are also shown. Error bars represent standard deviation ($n = 3$).

density, indicating the NEB followed apparent zero-order kinetics. It should be mentioned that before we started the NEB experiment, all samples in the ampules were kept at room temperature and there was a lag period before the samples reached the experimental temperatures, especially when the low temperatures were used. Time, however, was recorded from the exposure of samples to experimental temperatures. Slopes of the linear regression lines for all samples were used as rate constants (k). The coefficients of determination of the reaction rate constants (R^2) varied from 0.9425 to 0.9990. Representative examples of OD against time are shown in **Figure 3**. The kinetic data in the present study were slightly different from those reported by Lievonen and co-workers (*9*, *12*) for maltodextrin- and polyvinylpyrrolindone-based food models. They found that

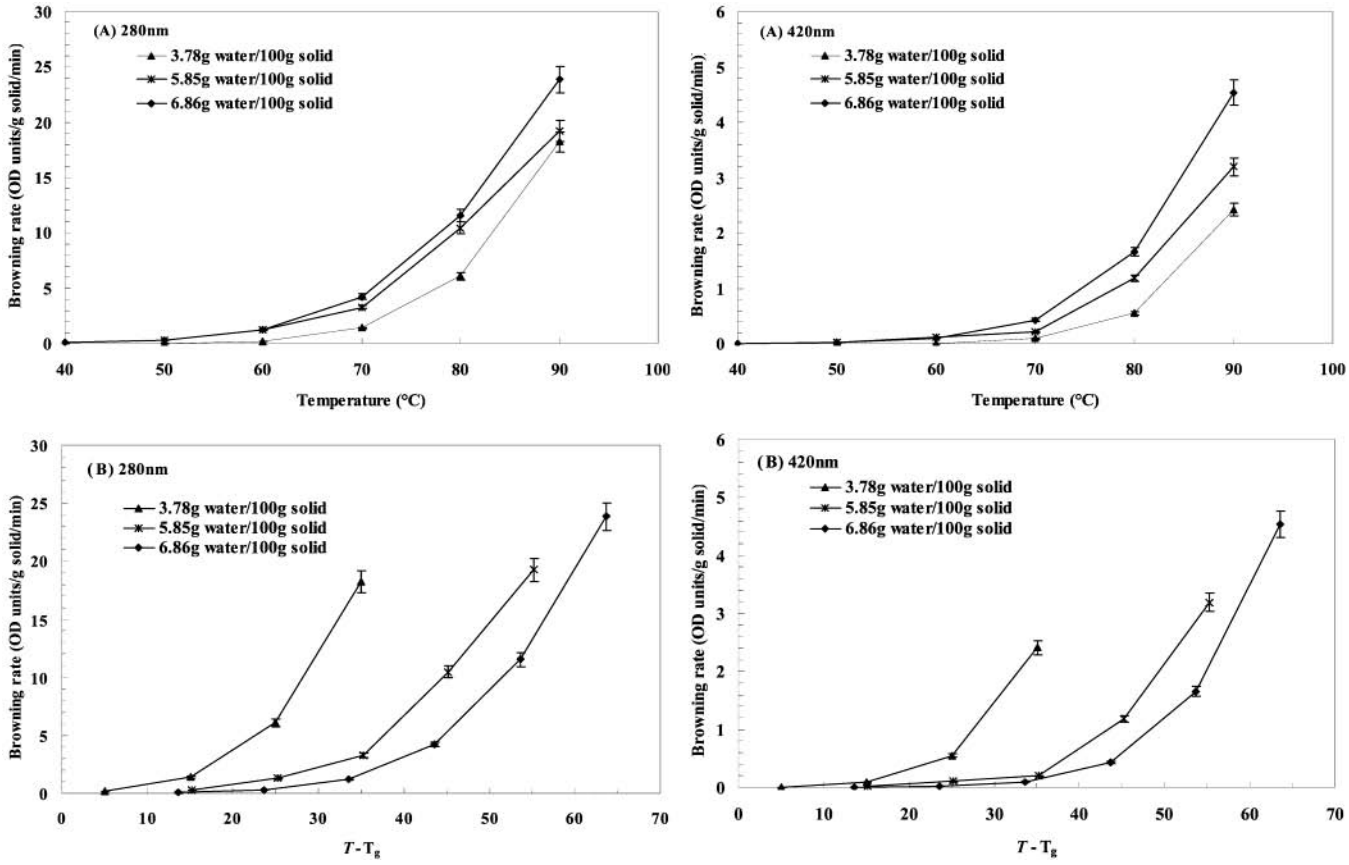

Figure 4. Effect of water content and (**A**) temperature or (**B**) temperature difference ($T-T_g$) on browning rate constants of the lactose/trehalose/reactant model. Rate constants at 280 nm and 420 nm are shown. Error bars represent the 95% confidence limits

the OD first increased linearly but leveled at a plateau as the reaction proceeded.

Nonenzymatic browning rates at all selected temperatures increased as the water content of the model increased (**Figure 4A**). At the low-temperature range close to glass transition, the difference of the rate constants due to different water contents became smaller; the NEB rate seemed to be less water content dependent. As the reaction rates were plotted as a function of the temperature difference $T - T_g$ (**Figure 4B**), the rate constant significantly increased with increasing $T - T_g$, as has been reported earlier (*6*, *9*, *19*, *22*, *24*). The models having the lowest water contents at all temperatures had the highest reaction rate dependence on $T - T_g$. In agreement with previous studies (*9*, *19*, *21*) of browning data for vegetables and food models, our results showed that the increase in browning rate as a function of $T - T_g$ was different at each water content and water activity, suggesting a strong dependence of the reaction rate on water and temperature. Increasing water contents may increase local T_g differences, moisture migration, plasticization, and reaction rate. In Figure 4A at constant temperature, the effect of water on the rate was not very large, but the rate increased slightly as water content increased. However, as shown in Figure 4B at constant $T - T_g$, there was a large dependence of the rate on water content, and the highest rate was observed for the lower water content. Temperature at a constant $T - T_g$ was much higher for systems with lower water content. While a small increase in the water content may increase browning, a small increase in temperature will result in a higher increase in browning. In the present study, most experimental temperatures were above the T_g. It seems that there was at each water content a critical $T - T_g$ value (Figure 4B) above which the rate increased rapidly. At lower temperatures, the rate was low and increased significantly at 15−30 °C above the T_g. This agreed with the results of Karmas et al. (*19*) and Lievonen et al. (*8*, *12*). They reported that an increase of nonenzymatic browning rate of intermediate-moisture systems was detected at a range of 10−40 °C above the T_g.

At spray-drying conditions, the temperature of the dry particle in the final dehydration stage may be higher than 70 °C. At that stage, the water contents of the particles are rapidly decreasing, which results in the increase of T_g. Much attention should be paid to prevention or control of the browning at the final stages of drying. Especially at the later stages of spray drying, the final moisture content of a dairy product may be higher than 4%, and if lactose is the T_g domain component, it can be assumed that the $T - T_g$ of the product may be higher than 40 °C. Hence, browning may become critical for quality changes resulting from drying.

Temperature Dependence. The nonenzymatic browning reaction has often been considered to follow zero-order kinetics, and the temperature dependence has been modeled with the Arrhenius equation (*4*, *5*, *8*, *21*, *45*, *46*). The temperature dependence of NEB in the food model system was analyzed using the Arrhenius relationship (*5*). According to the Arrhenius equation, a linear relationship exists between ln k and $1/T$. The rate of NEB in food models with different water contents could be modeled using Arrhenius equation, as shown in **Figure 5**. The Arrhenius plots agreed well with the data reported by Karmas et al. (*19*) and Lievonen et al. (*12*). Because most of the experimental temperatures were above the T_g, no break in the vicinity of the glass transition temperature could be observed. Only the model with 3.78 g of water/100 g of solids had a glass transition of 55.0 °C, and the in present study, nonenzymatic browning could still be observed at 40 and 50 °C, although the

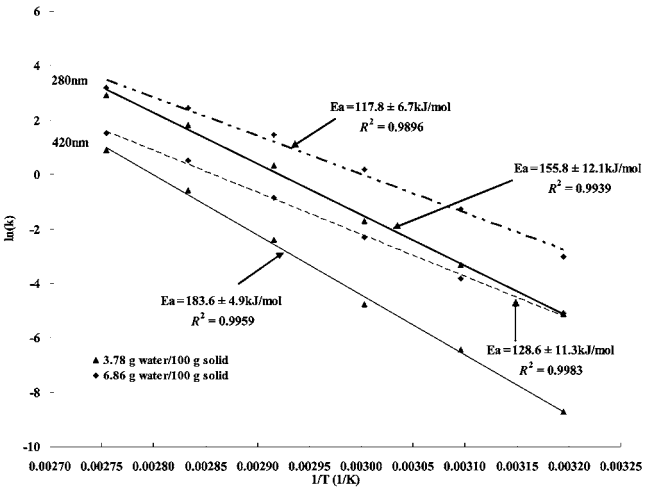

Figure 5. Arrhenius plots for NEB in freeze-dried lactose/trehalose models with different water contents as determined from optical density at 280 and 420 nm.

rate constant became very small. The results indicated that nonenzymatic browning may occur in highly viscous glassy materials. In agreement with the results reported by Karmas et al. (*19*), Schebor et al. (*47*), and Lievonen and Roos (*9*), however, a macroscopic T_g cannot be considered as an absolute threshold of food stability (*48*). Rotational mobility, aging of the glassy material, and diffusion through pores or defects of the glasses may explain the occurrence of chemical reactions in the glassy state (*47*) as well as local heterogeneities in water and reactant distribution, which are extremely likely in food systems.

The activation energy of the NEB reaction was calculated for each model. The activation energies of different model systems varied from 117.8 to 183.6 kJ/mol, and they were typical of the NEB reaction (*5*, *49*). As shown in **Figure 5**, when the water content in the food model varied from 3.8 to 6.9 g of water/100 g of dry solids, the activation energy changed from 155.8 to 117.8 kJ/mol. The water content seemed to affect the activation energy of NEB, which was probably because of a higher amount of water changed the physical state of the model and affected the diffusion rate and solute mobility in the system (*50*, *51*), thus lowering the NEB activation energy. From the Arrhenius plot in Figure 5, we could also observe that higher water contents seemed to decrease the temperature dependence of NEB rate. At the higher temperatures, the NEB rate increased, but the difference of the ln *k* between different water content models became smaller. This suggested that at the high temperatures the NEB rates were high and became less water content dependent. This should be considered in adjusting spray-drying conditions at later stages of the process.

Above T_g, increasing diffusion may be related to decreasing viscosity, and instead of using the Arrhenius type temperature dependence of reaction rate, the Williams−Landel−Ferry equation (WLF) (*52*) has been suggested as an alternative model to describe the temperature dependence of viscosity-controlled chemical reactions above the glass transition (*12*, *14*, *19*, *46*, *53*). Many authors have fitted the WLF equation to NEB data (*8*, *12*, *15*, *19*, *22*, *53*). Williams et al. (*52*) reported universal values for the constants $C_1 = -17.44$ and $C_2 = 51.6$. These values were also applied to describe the temperature dependence of viscosity of sugar solutions (*54*) and time to crystallization of amorphous sugars above T_g (*21*). Peleg (*55*) discussed several problems associated with the use of the universal constants in the WLF equation. He found disagreement between the use of

Table 4. WLF Coefficients of the Model Food System at 280 nm

water content (g water/100 g solid)	T_g	T_{ref}	T_g as ref temp			T_{ref} as ref temp		
			C_1	C_2	R^2	C_1'	C_2'	R^2
3.78	55.0	60	8.1	87.3	0.9995	5.3	49.6	1.0000
5.85	34.8	50	9.7	149.3	0.9876	4.3	56.6	0.9928
6.86	26.4	40	16.6	229.1	0.9891	8.0	95.4	0.9998

universal constants and the calculated constants for prediction purposes at 20−30 °C above the glass transition temperature. Lievonen et al. (*12*) confirmed that a better fit was found when system-dependent constants were calculated instead of using the universal constants. In the present study, the WLF constants C_1 and C_2 were calculated by use of the linear forms of eq 2 and eq 3.

$$\left[\log\frac{k_{ref}}{k}\right]^{-1} = \frac{-C_2}{C_1(T - T_{ref})} - \frac{1}{C_1} \quad (2)$$

$$\left[\log\frac{k_g}{k}\right]^{-1} = \frac{-C_2'}{C_1'(T - T_g)} - \frac{1}{C_1'} \quad (3)$$

where k_{ref}, k_g, and k are reaction rate constants at reference temperature T_{ref}, glass transition temperature T_g, and observation temperature T, respectively, as suggested by Nelson and Labuza (*46*). The experimental temperature closest to the predicted glass transition temperature was chosen as the reference temperature, and the reaction rate at glass transition temperature, k_g, was derived using the Arrhenius equation. A plot of ln *k* versus 1/*T* gave the k_o and E_a value in the Arrhenius equation. Then, from the predicted T_g, the k_g was obtained. The system-specific constants are given in **Table 4**. These WLF constants differed from the "universal" constants. The temperature dependence of the nonenzymatic browning of the model systems with different water contents could be modeled by use of the WLF equation (**Figure 6**). The WLF equation gave a good fit over the experimental temperature and water content ranges, but the calculated constants and the suitability of the WLF model varied significantly even at minor water content differences. This result gave further evidence against the use of the universal WLF constants and agreed with the results of Lievonen et al. (*12*). In a previous study, Nelson and Labuza (*46*) found that the WLF equation could be fitted to browning data, found for a carbohydrate model system by Karmas et al. (*19*) above T_g. It may be assumed that the rate constant for a diffusion-controlled reaction may follow WLF kinetics above T_g, provided that the reaction would occur with a significantly higher rate at the same temperature in a nondiffusion-controlled situation (*15*). Probably, the NEB reaction in the lactose/trehalose/reactant system was diffusion-controlled. Although structural changes in the present study, such as collapse, may have affected the browning rate, as was pointed out by Karmas et al. (*19*), such changes are related to viscosity, which in amorphous materials may be assumed to follow the WLF-type temperature dependence. Thus, the temperature dependence of the apparent NEB rate was in agreement with the WLF kinetics.

In conclusion, the NEB browning kinetics in the present study were obtained for a freeze-dried food model system at water contents and temperatures applicable to spray-drying conditions. The rates of browning in the food model were sensitive to water content and temperature and followed WLF kinetics, but the WLF constants were dependent on the water content. At temperatures above T_g, the Arrhenius model was applicable and

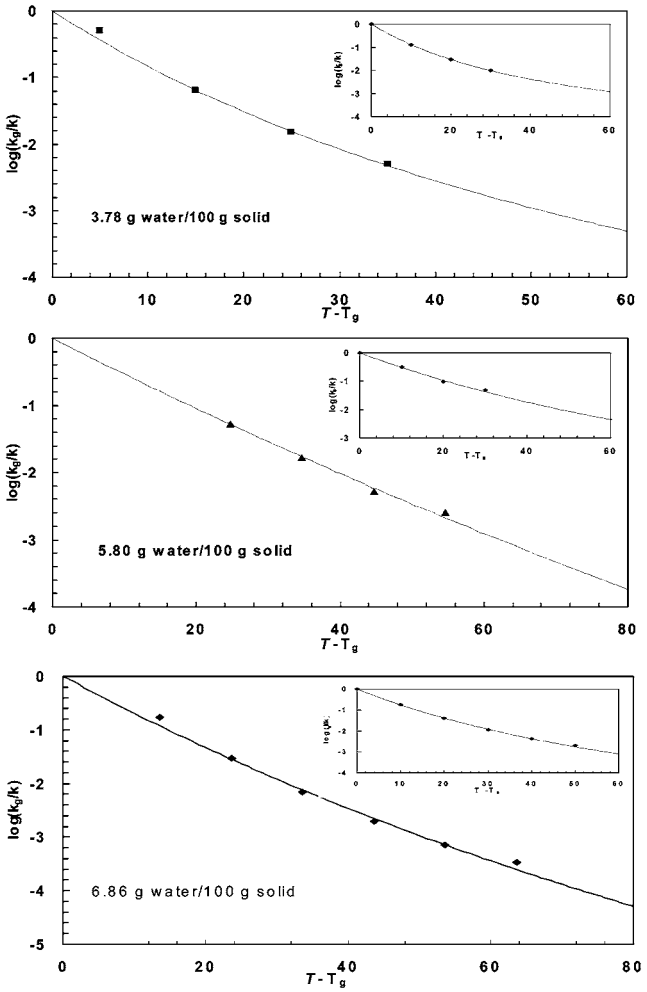

Figure 6. WLF plot of the NEB rate constant, k, as a function of the temperature difference between the sample temperature and the T_g of the model system at different water contents for freeze-dried L/T/R model system. The T_g of the system was predicted by use of a Gordon and Taylor equation and GAB model. The rate constant, k_g, at T_g was derived by use of the Arrhenius relationship. The inset figure shows the relation using another reference temperature, T_s, and an experimental value for the rate constant k_s at T_s.

linearity was observed. Water content seemed to affect the activation energy of NEB, and higher water contents decreased the temperature-dependence of NEB. At lower temperatures close to T_g, the NEB rate was low and more water content dependent. The results can be used to control NEB by water content and temperature, for example, in dehydration such as spray drying applications. To evaluate the NEB kinetics in real spray-drying conditions, however, future studies are necessary to compare the browning kinetics of the freeze-dried model and a spray-dried model.

LITERATURE CITED

(1) Morttram, D. S. Flavor compounds formed during the Maillard reaction. In *Thermally Generated Flavours*; Parliamnet, T. H., Morello, M. J., McGorrin, R. J., Eds.; American Chemical Society: Washington, D. C., 1994, pp 104−126.

(2) Friedman, M. Food browning and its prevention: an overview. *J. Agric. Food Chem.* **1996**, *44*, 631−653.

(3) O'Brien, J. Reaction chemistry of lactose: nonenzymatic degradation pathways and their significance in dairy products. In *Advance Dairy Chemistry*; Fox, P. F., Ed.; Chapman and Hall: London, U.K., 1997; pp 155−231.

(4) Labuza, T. P.; Saltmarch, M. The nonenzymatic browning reaction as affected by water in foods. In *Water Activity: Influences on Food Quality*; Rockland, L. B., Stewart, G. F., Eds.; Academic Press: New York, 1981, pp 605−650.

(5) Labuza, T. P.; Braisier, W. M. The kinetics of nonenzymatic browning. In *Physical Chemistry of Foods*; Schwartzberg, H. G., Hartel, R. W., Eds.; Marcel Dekker Inc.: New York, 1992; pp 595−649.

(6) Buera, M. P.; Karel, M. Effect of physical changes on the rates of nonenzymatic browning and related reaction. *Food Chem.* **1995**, *52*, 167−173.

(7) Bell, L. N.; White, K. L.; Chen, Y. H. Glycine loss and Maillard browning as related to the glass transition in a model food system. *J. Food Sci.* **1998**, *63*, 625−628.

(8) Lievonen, S. M.; Laaksonen, T. J.; Roos, Y. H. Glass transition and reaction rates: nonenzymatic browning in glass and liquid systems. *J. Agric. Food Chem.* **1998**, *46*, 2778−2784.

(9) Lievonen, S. M.; Roos, Y. H. Nonenzymatic browning in amorphous food models: effects of glass transition and water. *J. Food Sci.* **2002**, *67*, 2100−2106.

(10) White, K. L.; Bell, L. N. Glucose loss and Maillard browning in solids as affected by porosity and collapse. *J. Food Sci.* **1999**, *64*, 1010−1014.

(11) Burin, L.; Jouppila, K.; Roos, Y.; Kansikas, J.; Buera, M. P. Color formation in dehydrated modified whey powder systems as affected by compression and T_g. *J. Agric. Food Chem.* **2000**, *48*, 5263−5268.

(12) Lievonen, S. M.; Laaksonen, T. J.; Roos, Y. H. Nonenzymatic browning in food models in the vicinity of glass transition: effects of fructose, glucose, and xylose as a reducing sugar. *J. Agric. Food Chem.* **2002**, *50*, 7034−7041.

(13) Roos, Y.; Karel, M. Phase transition of mixtures of amorphous polysaccharides and sugars. *Biotechnol. Prog.* **1991**, *7*, 49−53.

(14) Slade, L.; Levine, H. Beyond water activity: recent advances based on an alternative approach to the assessment of food quality and safety. *Crit. Rev. Food Sci. Nutr.* **1991**, *30*, 115−359.

(15) Roos, Y. H.; Jouppila, K.; Zielasko, B. Nonenzymatic browning-induced water plasticization. Glass transition temperature depression and reaction kinetics determination using DSC. *J. Therm. Anal.* **1996**, *47*, 1437−1450.

(16) Champion, D.; Le Meste, M.; Simatos, D. Towards an improved understanding of glass transition and relaxations in foods: molecular mobility in the glass transition range. *Trends Food Sci. Technol.* **2000**, *11*, 41−55.

(17) Echner, K.; Karel, M. The influence of water content and water activity on the sugar-amino browning reaction in model systems under various conditions. *J. Agric. Food Chem.* **1972**, *20*, 218−223.

(18) Slade, L.; Levine, H. Glass transition and water−food structure interactions. *Adv. Food and Nutr. Res.* **1995**, *38*, 103−269.

(19) Karmas, R.; Buera, M. P.; Karel, M. Effect of glass transition on rates of nonenzymatic browning in food systems. *J. Agric. Food Chem.* **1992**, *40*, 873−879.

(20) Craig, I. D.; Parker, R.; Rigby, NM.; Crairns, P.; Ring, S. G. Maillard reaction kinetics in model preservation system in the vicinity of glass transition: experiment and theory. *J. Agric. Food Chem.* **2001**, *49*, 4706−4712.

(21) Karmas, R.; Karel, M. The effect of glass transition on Maillard browning in food models. In *Maillard Reactions in Chemistry, Food, and Health*; Labuza, T. P., Reineccius, G. A., Monnier, V. M., O'Brien, J., Baynes, J. W., Eds.; The Royal Society of Chemistry: Cambridge, U.K., 1994; pp 182−187.

(22) Roos, Y. H.; Himberg, M. J. Nonenzymatic browning behaviour, as related to glass transition of a food model at chilling temperatures. *J. Agric. Food Chem.* **1994**, *42*, 893−898.

(23) Schebor, C.; Buera, M. P.; Karel, M.; Chirife, J. Color formation due to nonenzymatic browning in amorphous, glassy, anhydrous model systems. *Food Chem.* **1999**, *65*, 427−432.

(24) Bell, L. N. Kinetics of nonenzymatic browning in amorphous solid systems: distinguishing the effects of water activity and the glass transition. *Food Res. Int.* **1996**, *28*, 591−597.
(25) Lievonen, S. M.; Roos, Y. H. Water sorption of food models for studies of glass transition and reaction kinetics. *J. Food Sci.* **2002**, *67*, 1758−1766.
(26) Greenspan, L. Humidity fixed points of binary saturated aqueous solution. *J. Res. Natl. Bur. Stand., Phys. Chem.* **1977**, *81A*, 89−96.
(27) Labuza, T. P.; Kaanane, A.; Chen, J. Y. Effect of temperature on the moisture sorption isotherms and water activity shift of two dehydrate foods. *J. Food Sci.* **1985**. *50*, 385−391.
(28) Brunauer, S.; Emmett, P. H.; Tellet, E. Adsorption of gases in multimolecular layers. *J. Am. Chem. Soc.* **1938**, *60*, 309−319.
(29) Roos, Y. H. Water activity and physical state effects on amorphous food stability. *J. Food Process. Preserv.* **1993**, *16*, 433−447.
(30) van den Berg, C.; Bruin, S. Water activity and its estimation in food systems: Theoretical aspects. In *Water Activity: Influences on Food Quality*; Rockland, L. B., Stewart, G. F., Eds.; Academic Press: New York, 1981; pp1−61.
(31) Jouppila, K.; Roos, Y. H. Water sorption and time-dependent phenomena of milk powders. *J. Dairy Sci.* **1994**, *77*, 1798−1808.
(32) Gordon, M.; Taylor, J. S. Ideal copolymers and the second-order transitions of synthetic rubbers. I. Noncrystalline copolymers. *J. Appl. Chem.* **1952**, *2*, 493−500.
(33) Johari, G. P.; Hallbrucker, A.; Mayer, E. The glass−liquid transition of hyperquenched water. *Nature* **1987**, *330*, 552−553.
(34) Roos, Y. H. In *Phase Transitions in Foods*; Academic Press.: San Diego, C.A., 1995; p 360.
(35) Flink, J. M. Nonenzymatic browning of freeze-dried sucrose. *J. Food Sci.* **1983**, *48*, 539−542.
(36) Hodge, J. E.; Osman, E. M. Carbohydrates. In: *Principle of Food Science*; Fennema, O. R., Ed.; Dekker: New York, 1976; pp 41−138.
(37) Resnik, S.; Chirife, J. Effects of moisture and temperature on some aspects of nonenzymatic browning in dehydrated apple. *J. Food Sci.* **1979**, *44*, 601−605.
(38) Whistler, R. L.; Daniel, J. R. Carbohydrates. In *Food Chemistry*, 2nd ed.; Fennema, O. R., Ed.; Dekker: New York, 1985; pp 69−137.
(39) Labuza, T. P. Application of chemical kinetics to deterioration of foods. *J. Chem. Educ.* **1984**, *61*, 348−358.
(40) Berlin, E.; Anderson, B. A.; Pallansch, M. J. Water vapour sorption properties of various dried milks and whey. *J. Dairy Sci.* **1968**, *51*, 1339−1344.
(41) Lai, H.; Schmidt, S. J. Lactose crystallization in skim milk powder observed by hydrodynamic equilibria, scanning electron microscopy, and ^{2}H nuclear magnetic resonance. *J. Food Sci.* **1990**, *55*, 994−999.
(42) Arvanitoyannis, I.; Blanshard, J. M. V. Rate of crystallization of dried lactose-sucrose mixtures. *J. Food Sci.* **1994**, *59*, 197−205.
(43) Biliaderis, C. G.; Lazaridou, A.; Mavropoulos, A.; Barbayiannis, N. Water plasticizing effects on crystallization behaviour of lactose in a co-lyophilized amorphous polysaccharide matrix and its relevance to the glass transition. *Int. J. Food Prop.* **2002**, *5* (2), 463−482.
(44) Warmbier, H. C.; Schnickel, R. A.; Labuza, T. P. Effect of glycerol on nonenzymatic browning in a solid intermediate moisture model food system. *J. Food Sci.* **1976**, *41*, 528−531.
(45) Labuza, T. P. The effect of water activity on reaction kinetics of food deteriation. *Food Technol.* **1980**, *34* (4), 36−41, 59.
(46) Nelson, K. A.; Labuza, T. P. Water activity and food polymer science: implication of state on Arrhenius and WLF models in predicting shelf life. *J. Food Eng.* **1994**, *22*, 271−289.
(47) Schebor, C.; Buera, M. P.; Karel, M.; Chirife, J. Color formation due to nonenzymatic browning in amorphous, glassy, anhydrous model systems. *Food Chem.* **1999**, *65* (4), 427−432.
(48) Simatos, D.; Blond, G.; Pérez, J. Basic physical aspects of glass transitions. In *Food Preservation by Moisture Control*; Barbosa-Cánovas, G. V., Welti-Chanes, J., Eds.; Technimic: Lancaster, PA, 1995; pp 3−31.
(49) van Boekel, M. A. J. S. Kinetic aspects of the Maillard reaction: a critical review. *Nahrung* **2001**, *45*, 150−159.
(50) Duckworth, R. B. Solute mobility in relation to water content and water activity. In *Water Activity: Influences on Food Quality*; Rockland, L. B., Stewart, G. F., Eds.; Academic Press: New York, 1981; pp 295−317.
(51) Sherwin, C. P.; Labuza, T. P.; McCormick, A.; Chen, B. Cross-polarization/magic angle spinning NMR to study glucose mobility in a model intermediate-moisture food system *J. Agric. Food Chem.* **2002**, *50*, 7677−7683.
(52) Williams, M. L.; Landel, R. F.; Ferry, J. D. The temperature dependence of relaxation mechanisms in amorphous polymers and other glass-forming liquids. *J. Am. Chem. Soc.* **1955**, *77*, 3701−3707.
(53) Buera, M. P.; Karel, M. Application of the WLF equation to describe the combined effects of moisture and temperature on nonenzymatic browning rate in food systems. *J. Food Process. Preserv.* **1993**, *17*, 31−45.
(54) Soesanto, T.; Williams, M. C. Volumetric interpretation of viscosity for concentrated and dilute sugar solutions. *J. Phys. Chem.* **1981**, *85*, 3338−3341.
(55) Peleg, M. On the use of the WLF model in polymers and foods. *Crit. Rev. Food Sci. Nutr.* **1992**, *32*, 59−66.

Received for review February 22, 2004. Revised manuscript received May 27, 2004. Accepted June 6, 2004. This study was carried out with the financial support of PRTL1 Cycle 3 of the Higher Education Authority of Ireland.

JF049706T